The SPASIBA Force Field for Chondroitin Sulfate: Vibrational Analysis of D-Glucuronic and *N*-acetyl-D-Galactosamine 4-Sulfate Sodium Salts

M. Meziane-Tani,[†] P. Lagant,[‡] A. Semmoud,[§] and G. Vergoten*[,‡]

Département de Biologie, Faculté des Sciences, Université Abou Bekr Belkaid, 22 rue Abi Ayed Abdelkrim, Faubourg Pasteur, 13000 Tlemcen, Algérie, UMR 8576 CNRS Glycobiologie Structurale et Fonctionnelle, Université des Siences et Technologies de Lille, Bâtiment C9, 59655 Villeneuve D'Ascq, France, and LASIR Université des Sciences et Technologies de Lille, Bât C8, 59655 Villeneuve D'Ascq, France

Received: June 21, 2006

Normal-mode analyses were carried out on the two components of the chondroitin 4-sulfate linear glycosaminoglycan, a copolymer implying alternate D-glucuronate β-(1→3) and *N*-acetyl-D-galactosamine 4-sulfate β-(1→4) (hereafter named D-galactosamine 4-sulfate) residues. Scaled quantum mechanical calculations (SQM) using the density functional theory approach at different levels of theory (B3LYP/6-31G** and B3LYP/6-31++G**) were performed to obtain correct vibrational assignments. The SPASIBA empirical force field parameters were then obtained from both theoretical predictions and observed IR and Raman data. It is shown that calculations including diffuse functions at the B3LP/6-31++G** level and the introduction of the Na+ counterion are necessary to give correct assignments of the CO2− symmetric (ν_s) and antisymmetric (ν_a) stretching modes for the glucuronic carboxylate residue.

I. Introduction

Glycosaminoglycans (GAG) form an important part of cartilage, displaying large swellings in aqueous solutions containing Na^+ or Ca^{2+} cations and conformational properties originating from their interactions with the carboxylate and sulfate groups present all along the polymeric chain and between neighboring molecules. Chondroitin sulfate (CS) and hyaluronic acid (HA) have been the center of a large number of conformational studies involving vibrational (infrared and Raman, infrared dichroism) spectroscopies[1] or molecular dynamics studies to measure effects of water and counterions on the overall dynamics properties of cartilage.[2,3] Chondroitin 4-sulfate (CS4) exhibits alternating dimers of pyranose rings containing carboxylate (β1→3 D-glucuronic) or sulfate (*N*-acetyl D-galactosamine β1→4) groups. The crystalline conformations of chondroitin sulfate in the presence of counterions were derived by Winter et al.[4] and by Cael et al.[5]

As a consequence of the local environments of carboxylate and sulfate groups upon the presence of Na^+ or Ca^{2+} ions, this copolymer can adopt different molecular conformations such as helical structures.[6−8] The conformational dependence of this polymer versus the degree of hydration was also largely investigated.[9]

The present purpose was to get derived empirical force field parameters for further conformational studies, such as molecular dynamics in the natural environment (water and counterions). The empirical SPASIBA force field allows these parameters to be obtained from spectroscopic vibrational data and applied to the D-glururonate and D-galactosamine 4-sulfate anions treated first as isolated species and then in the presence of Na^+ counterions.

* Corresponding author. E-mail: gerard.vergoten@univ-lille1.fr.
[†] Université Abou Bekr Belkaid.
[‡] CNRS.
[§] LASIR.

II. Methodology

II.a. Vibrational Spectra. Due to the instability of D-galactosamine 4-sulfate sodium salt at room temperature, no experimental data could be obtained for this compound.

The infrared spectrum of the D-glucuronate sodium salt in the solid-state form was recorded using an IR Avatar 360 Nicolet apparatus. Raman spectra were obtained using a Raman TF Bruker FS 100/s apparatus and the 1064-nm line of a Nd:YAG continuous laser with 140-mW power for a spectral resolution of 4 cm^{-1}.

II.b. Scaled Quantum Mechanical Calculations. The geometry optimizations and normal-mode analyses have been performed using the density functional theory (DFT) at different levels, B3LYP/6-31G** for the isolated anion species and B3LYP/6-31++G** when in the presence of a sodium counterion using the *Jaguar* program[10] (see Supporting Information for data). The optimized Hessian matrix was then translated to the internal coordinate space, leading to the possibility of applying scaling factors to the internal force constants in fitting the theoretical wavenumbers to the experimental ones using least-squares methods. This part was done using the *Redong* program of Allouche and Pourcin.[11]

At this level of DFT calculations, a general scaling factor of 0.96−0.98 is usually recommended to simulate correctly the experimental vibrational frequencies and to obtain an adequate potential energy distribution (PED) among internal coordinates.[12]

II.c. Empirical Force Field. The SPASIBA force field is a spectroscopic molecular-mechanics-derived empirical potential function first devoted to proteins[13] and extended to a large variety of chemical groups such as alkanes, alkenes, amino acids, ethers, esters, thiols, alcohols, saccharides, and phospholipids.[14−20] Not only does this force field appear to be an adequate tool for molecular mechanics studies of monosaccharides, but it has also been extended to force constant determination related to various glycosidic linkages along the establishment of Ramachandran's ϕ, ψ maps.[14,15]

10.1021/jp063862g CCC: $33.50
Published on Web 09/14/2006

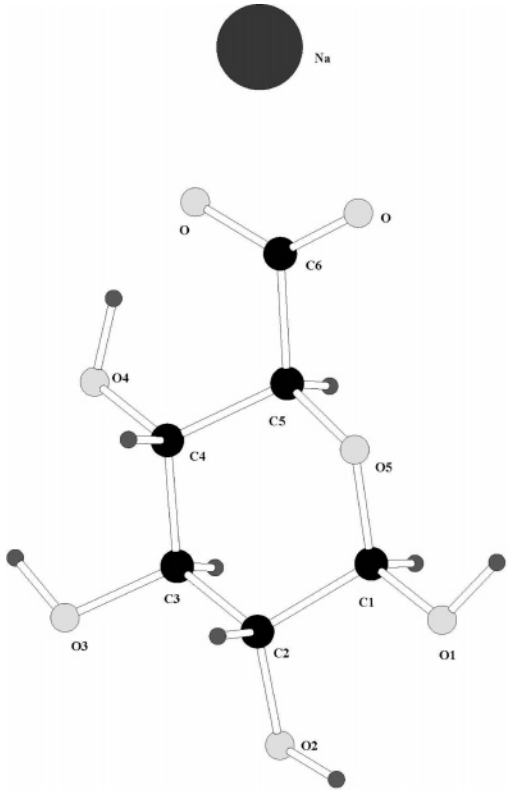

Figure 1. D-Glucuronic acid sodium salt (ball-and-stick representation).

The SPASIBA force field has been developed in our group for many years. It is able to reproduce at the same time structures energies and vibrational spectra with a much higher precision on the latter than commonly available force fields. This is the main reason it has recently been introduced into the *CHARMM* package.[15] Therefore, the SPASIBA force field is a molecular force field which can be used with high confidence, particularly in molecular dynamics simulations where it has to be reliable over the whole potential energy surface rather than in the vicinity of the minima, since the parameters deduced from spectra reflect the curvature of the potential surface. The philosophy of SPASIBA and all the procedures for parameter determination have been given in detail in a series of papers corresponding to thermally excited modes (see refs 13−15 and references therein). In particular, in addition to the classical quadratic parameters *K* (bond stretching coordinate) and *H* (bond angle bending coordinate), SPASIBA introduces the Urey−Bradley *F* quadratic force constant related to the 1−3 nonbonded distance in a bond angle, solves the redundancy problem among internal coordinates, and adds specific parameters to correctly fit spectra (see ref 14 and Table 7). Special interest has been devoted to the low-wavenumber spectral range (10−200 cm^{-1}) corresponding to thermally excited modes. These modes are of large amplitude and reflect molecular flexibility. In this spectral range, coupled modes are found mainly corresponding to torsional coordinates and/or eventually mixed with in-plane and out-of-plane angular bending coordinates and sometimes even more stretching coordinates (longitudinal and transverse acoustical vibrations of long-chain molecules.[21,22] Assuming a functional form for the internal rotation potential (a Fourier series), the various barriers to internal rotation *Vn* (Table 7) may be deduced from the experimental and/or theoretical spectra. This was particularly done for carbohydrates and the glycosidic linkages.[23−26]

TABLE 1: Geometry Parameters Derived from DFT and Semiempirical Geometry Optimizations for the Sodium Salt Form of Glucuronic Acid Taken as an Isolated Anion[a] or in Presence of Its Counterion[b]

internal coordinates[c]	DFT(6-31G**)[a]	DFT(6-31++G**)[b]	SPASIBA
C1−O5	1.402	1.416	1.412
C5−O5	1.438	1.422	1.44
C1−C2	1.531	1.537	1.529
C2−C3	1.525	1.529	1.521
C3−C4	1.526	1.535	1.54
C4−C5	1.537	1.535	1.552
C5−C6	1.566	1.532	1.516
C1−O1	1.411	1.399	1.434
C2−O2	1.423	1.418	1.433
C3−O3	1.423	1.420	1.434
C4−O4	1.408	1.418	1.449
C6−O1	1.236	1.257	1.245
C6−O2	1.278	1.284	1.249
C5C6O1	118.6	116.5	119.9
C5C6O2	112.2	120.1	119.8
O1−C6−O2	129.2	123.4	120.1
C1−O5−C5	111.7	112.1	113.9
H1,C1−O1,HO1	80.9	64.6	131.1
H2,C2−O2,HO2	−67.0	−60.4	−92.1
H3,C3−O3,HO3	−79.3	−68.9	−85.5
H4,C4−O4,HO4	81.0	71.3	86.4
C4,C5−C6,O1	141.3	146.2	91.1
O5,C5−C6,O1	19.5	24.2	−24.1
C4,C5−C6,O2	−40.9	−35.3	−94.0
O5,C5−C6,O2	−162.7	−157.4	150.85
HO4····O2	1.602	1.861	1.96
C4−O4−HO4	100.5	105.1	107.4
O4−HO4···O2	153.1	140.2	136.9
C4,O4−HO4,O2	10.7	19.8	3.7
O1···Na		2.19	
O2···Na		2.20	
C6O1−O2Na		180.	

[c] Distances are given in angstroms and angles in degrees.

III. Results and Discussion

III.a. D-Glucuronic Acid Sodium Salt. The sodium salt of glucuronic acid was first investigated as an anionic moiety without participation of the Na^+ counterion (Figure 1). A B3LYP geometry optimization was performed using the 6-31G** basis set, and final geometrical parameters can be examined in Table 1. As ab initio or DFT-derived vibrational wavenumbers currently display overestimated values than experimental ones, the Cartesian F_X matrix was transformed into the internal coordinate space before scaling of the force constants via the *Redong* program.[11] A general scaling factor of 0.962 was first applied to every internal coordinate force constant, as, generally, such a value leads to correct vibrational wavenumbers and assignments of the normal modes. However, in the present case, the localization of the symmetric stretching mode of the carboxylate group appears quite appalling. As can be noted from examination of the optimized geometry parameters, one of the carboxylate oxygens undergoes a hydrogen bond with the O4 hydroxyl hydrogen atom ($H\cdots O_{CO2}$ = 1.602 Å; $O4-H\cdots O_{CO2}$ = 153°) leading to a longer length value for the implied C−O carboxylate bond, 1.27 Å, as compared to the free C−O one (1.236 Å).

A surprisingly low scaling factor of 0.89 had to be applied to the force constants related to the internal C−O stretching coordinates to correctly locate the antisymmetric stretching mode (ν_a) of the $CO2^-$ group (calculated here at 1584 cm^{-1}), while an anomalously low wavenumber (1195 cm^{-1}) was theoretically obtained here for the symmetric ν_s(CO2) mode in place of the experimental value, generally expected in the 1320−1390 cm^{-1}

TABLE 2: Vibrational Wavenumbers as Obtained from DFT Calculations at the B3LYP/6-31++G Level for the D-Glucuronic Sodium Salt in Presence of the Na^+ Counterion[a]**

Raman	IR	6-31G**	6-31++G**	potential energy distribution
		64.9	94.7	0.82τCTCT + 0.20τC5O5 + 0.08τC5C6
		77.6	108.7	0.70τCTCT + 0.17τC5O5 + 0.13τC5C6
		112.7	118.9	0.91τCTCT + 0.09τCTO5
146 vw		139.8	159.1	0.30τCTO5 + 0.25τC5O5 + 0.25τCTCT + 0.08δCTO5CT + 0.07δCTCTC6 + 0.05δC5H
170 vw		169.6		0.62τC1O1 + 0.27τCTCT + 0.26τCTO5
187 vw				
222 vw		239.1	241.4	0.40δC3O + 0.25δC2O + 0.13δO5C5C6 + 0.12δCTCTC6
246 vw		259.8	252.1	0.24δC1O1 + 0.20δC2O + 0.19δC2O + 0.10δC3O + 0.09δO5C5C6 + 0.09δC4O
			259.4	0.23δO5C5C6 + 0.16δC2O + 0.14δC3O + 0.13τC1O1 + 0.12δC1O1 + 0.12δCTCTC6
298 w		298.2	297.2	0.25τCTCT + 0.18δC2O + 0.14δC3O + 0.13τC1O1 + 0.11δC4O + 0.10τCTCT + 0.08δC3H
314 w		306.6	315.0	0.50δC4O + 0.17τC1O1 + 0.17δC4O + 0.08δCTCTC6 + 0.08δCTCTO5
			335.6	0.41τC1O1 + 0.15δC4O + 0.13δCTCTC6 + 0.10νC5C6 + 0.08δC1O1 + 0.08δO5C5C6
356.		342.3	359.7	0.48τC1O1 + 0.14νC5C6 + 0.13δCTO5CT + 0.11νCTCT + 0.07δCTCTCT
381 S			387.3	0.26τC2O + 0.20δCTCTO5 + 0.18τCTO5 + 0.18δC3O.10τCTCT + 0.09δC3O
		380.4		0.52 δCTH + 0.18dCTCTCT + 0.16δCTCTCT + 0.16δCTH
			399.3	0.64τC2O + 0.34δCTCTCT + 0.12δCTO5CT
423 S		417.2	417.8	0.62τC2O + 0.12δC1O1 + 0.10δC2O + 0.09δCTCTCT + 0.07νCTCT
		383.5	418.5	0.63δ(CCO) + 0.17νCTCT + 0.08δC4O + 0.07δC2O + 0.05δCTCTCT
452 S		485.0	447.9	1.00τC3O
470		399.9	454.7	0.31δ(CCO) + 0.23τC3O + 0.14νC5O5 + 0.12νCTCT + 0.10δCTCTCT + 0.10νC1O1
538			520.7	0.33δC3O + 0.21γ(CO2) + 0.13δC1O1 + 0.12τC5O5 + 0.11δC3H + 0.10δC2H
	569	559.0	573.8	0.34δCTCTO5 + 0.20νC2O + 0.16νC5C6 + 0.10δCTO5CT + 0.10νCTCT + 0.10δC2O
581	582	570.0	583.7	0.30δC4O + 0.26δC1O1 + 0.14δC2O + 0.11δC3O + 0.07δC2H + 0.06δC3H + 0.06δ(CCO)
615 sh	617	632.9	644.3	0.28δC1O1 + 0.21δ(CCO) + 0.17γ(CO2) + 0.16δC4O + 0.12δO5C5C6 + 0.06δC3O
681 w	677 S	664.8	687.1	0.86τC4O + 0.14γ(CO2)
740 w	733 VS	754.1	694.0	0.57τC4O + 0.16γ(CO2) + 0.11δ(CO2) + 0.08δ(CCO) + 0.08νC5C6
827 vw	834 m		800.8	0.36δ(CO2) + 0.33γ(CO2) + 0.25δ(CCO) + 0.07δO5C5C6 + 0.06ν(CO2)
903 vw	901 m	897.3	939.9	0.37νC5C6 + 0.25ν(CO2) + 0.12γ(CO2) + 0.09νCTCT + 0.08δ(CO2) + 0.08νC3O
957 w	960 m	976.3	990.8	0.49νCTCT + 0.12νC2O + 0.11νC4O + 0.11νC3O + 0.10νC1O1 + 0.08δC2OH
		981.0	996.9	0.31νCTCT + 0.14νC3O + 0.14νC2O + 0.12νC4O + 0.12νCTCT + 0.09δCTCTO5
1016 w	1019 VS	1005.1	1023.5	0.32νCTCT + 0.30νCTO5 + 0.18δC1OH + 0.09νC4O + 0.06δC2H + 0.05δCTO5CT
1035 w	1039 VS	1033.5	1048.3	0.38νCTO5 + 0.22νCTCT + 0.16νC5O5 + 0.09δC2O + 0.07δCTCTO5 + 0.07δCTO5CT
1054 w		1055.5	1069.9	.64νCTCT + 0.12νC4O + 0.08δCTCTO5 + 0.07νC2O + 0.07δC5H
1079 w	1068 VS	1071.1	1081.4	.27νC2O + 0.21νCTCT + 0.16νCTO5 + 0.16νC4O + 0.11νC5O5 + 0.08νC1O1
		1085.4	1086.8	.51νC3O + 0.12νC1O1 + 0.10νCTCT + 0.07δC2H + 0.07νCTCT + 0.07νC2O
	1113 S	1105.5	1106.5	0.39νC2O + 0.28νC4O + 0.26νC5O5 + 0.08νCTO5
1108 VS	1128 m	1112.8	1119.3	0.52νCTO5 + 0.28νC4O + 0.20νCTCT
1165	1163 S		1136.7	0.60νC1O1 + 0.32νC3O + 0.07δCTCTCT
1197 w	1192 w		1171.2	0.19νC1O1 + 0.17δC3H + 0.15δC3H + 0.13δC2H + 0.13δC2OH + 0.13δC3OH + 0.10δC1H
		1195.7		0.45 νS(CO2 +. 36δC5H + 0.18 δC2H
		1213.1		0.42 νs(CO2) + 0.39δCH + 0.19δC1O1H
		1222.8	1222.6	0.38δC1OH + 0.23δC1H + 0.09δC4H + 0.09δC1H + 0.09δC3H + 0.06δC2OH + 0.06δC2H
	1237	1239.7	1238.7	0.26δC5H + 0.22δC2OH + 0.12δC4H + 0.11δC4H + 0.11δC5H + 0.10δC2H + 0.07δC5H
1247	1254		1269.5	0.26δC3OH + 0.25δC3H + 0.18δC2H + 0.12δC3H + 0.10δC2OH + 0.09δC2H
			1273.6	0.39δC4H + 0.29δC5H + 0.19δC4O4H + 0.07δC1O1H + 0.06δC2H
1296.6	1297	1295.3	1293.2	0.72δC5H + 0.16δC1H + 0.11ν(CO2)
1316 m		1315.8	1309.2	0.33δC2H + 0.27δC2H + 0.22δC1OH + 0.18δC2OH
1332 m	1337 m	1337.9	1334.1	0.21δC4H + 0.20δC4OH + 0.16νC1H6 + 0.15δC3H + 0.12δC3H + 0.11δC3OH
		1349.2	1351.7	0.61δC1H + 0.16δC2OH + 0.16δC2H + 0.07δC3OH
			1357.1	0.44δC3H + 0.34δC4H + 0.14δC5H + 0.08δC4OH
1365 w sh	1364 (sh)	1366.4	1365.4	0.20δC3OH + 0.17δC2H + 0.15ν(CO2) + 0.14δC1H + 0.14νC1H6 + 0.11δC2OH
1365 m	1380 S		1391.4	0.36νs(CO2) + 0.21δC4OH + 0.10δC4H + 0.10νC5C6 + 0.10δC5H + 0.07δC1H + 0.07δC2H
		1403.7	1418.7	0.30δC1H + 0.25δC1H + 0.16δC1OH + 0.09νCTCT + 0.07δC2H + 0.07δC2H + 0.06ν(CO2)
1426	1424 S	1424.5	1430.7	0.18δC1H + 0.15δC1H + 0.15δC1OH + 0.15ν(CO2) + 0.14δC4OH + 0.12νC5C6

TABLE 2: Continued.

Raman	IR	6-31G**	6-31++G**	potential energy distribution
	1457 w		1439.4	0.33δC4OH + 0.15δC3H + 0.11δC3H + 0.11δC2H + 0.10δC2H + 0.10δC3OH + 0.09δC2OH
1457	1473 w	1468.2		0.48ν(CO2) + 0.42νCTCT + 0.15δC4H
	1520(sh)			
1569	1581 S	1584.8	1582.4	0.80va(CO2) + 0.10νCTCT + 0.05νC5C6 + 0.05δ(CCO)
1611 w				
1642 w				
	2736	2839	2888.3	1.00νC1H
	2795	2893	2901.1	1.00νC5H
2927	2847	2910	2925.9	0.74νC3H + 0.26νC4H
2903	2905	2870	2939.6	0.76νC4H + 0.24νC3H
2927	2930	2953	2969.0	1.00νC2H
	3139	2943	3507.3	1.00νO4H
3330	3333	3604	3620.6	1.00νO3H
	3472	3651.9	3641.3	1.00νO2H
	3597	3660.3	3647.6	1.00νO1H

[a] Corresponding predicted B3LYP/6-31G** wavenumbers are given when comparable potential energy distribution was found. Scaling factors for internal force constants: νC−O (scf = 0.97); νO−H (scf = 0.962); and all others (scf = 0.98). ν: stretching. δ: in-plane bending. γ: out-of-plane bending. τ: torsion. ν_s and ν_a: antisymmetic and symmetric stretching modes of the CO2 group. w: weak. m: medium. S: strong. VS: very strong. sh: shoulder.

range (Table 2). The low difference in bond lengths between the two C−O groups does not, in our minds, justify the use of a different scaling factor for each of them. However, this apparent large shift between the ν_a(CO2) and ν_s(CO2) normal modes will lead us to use diffuse functions and to examine the effects of the presence of a counterion in the neigborhood of the carboxylate group. This will be discussed below.

Several contributions to the out-of-plane wagging mode of the carboxylate group are predicted to occur at 665 and 883 cm^{-1}, and the δ(OCO) in-plane bending mode is mainly predicted at 754 cm^{-1} when keeping a general scaling factor of 0.962 for the B3LYP/6-3G**-type of calculations. These values have to be related to those obtained for the calcium malonate dihydrate as given by Brusau et al.,[27] i.e., 785 cm^{-1} δ(OCO), 605 cm^{-1} δ(CCO) predicted here at 632 cm^{-1}. These authors identified the ν_a and ν_s(CO2) modes to occur at 1565 and 1365 (and 1430) cm^{-1}, respectively.

III.a.1. Endocyclic Ring and Exocyclic Hydroxyl modes. The 1500−1200 cm^{-1} range appears as a region of complex coupled modes of vibrations involving hydrogen atoms (i.e., COH, HCO, CCH). In this range, the quantum mechanically derived δCH and δC−O in-plane deformations take place predominantly. These results support quite well the work of Dauchez et al.[23,25,26] performed on normal-mode investigations for mono- and disaccharides in the crystal forms.

The 1200−1000 cm^{-1} domain was confirmed by the last authors to imply principally νC−O and νC−C stretching modes. The present DFT calculations extend these assignments to a lower boundary of 900 cm^{-1}.

The 1000−600 cm^{-1} vibrational range is well-known to contain two distinct domains implying the so-called fingerprint and crystalline regions for monosaccharides in the crystal state.They exhibit vibrations originating from the hemiacetal group (C5O5C1O1), generally involving endocyclic in-plane bending modes, as calculated here at 559−570 cm^{-1} (δC2C1O5, δC2C1O1, and δCOC).

The theoretical DFT exocyclic δCCO modes are predicted in the range 260−380 cm^{-1} and correspond to the empirical force field determinations performed by Dauchez and co-workers.

The high-frequency modes including the O−H stretching modes are correctly predicted to occur in the 3400−3600 cm^{-1} range, apart from the O4−H stretching motion calculated at 2943 cm^{-1} when using the general scaling factor of 0.962. This mode is expected to appear at approximately 3130 cm^{-1} corresponding to a Raman and IR experimental value. This mode frequency certainly corresponds in the present model to a strong hydrogen bond taking place between one of the carboxylate oxygen atoms and the O4 hydroxyl hydrogen atom.

III.a.2. Use of Diffuse Functions. Implication of a Na$^+$ Counterion. Addition of diffuse functions to the basis sets has been shown to be essential for accurate analyses of compounds containing lone pairs or anions or when dealing with transition structures, but it produces only a few changes when applied to molecules such as sugars.[28]

Recently, Keresztury et al.[29] have shown that SQMFF-type calculations on the acetate ion at the B3LYP/6-31G* level were unable to explain the frequency splitting between the ν_a and ν_s modes of the carboxylate group. Furthermore, these authors pointed out the necessity to introduce a Na$^+$ counterion as a bidentate complex or as a water complex to obtain adequate vibrational descriptions of the antisymmetric and symmetric C−O stretching modes. They also used a polarizable continuum model (PCM) and were able to reproduce the experimental shift between these two modes.

In the present work, a B3LYP calculation using the 6-31++G** basis set involving diffuse functions was performed on the sodium salt form of D-glucuronic acid. The carboxylate anion now forms a bidentate complex with the sodium ion in the OCO plane at a distance of 2.2−2.4 Å from each carboxyl oxygen atom. Similar values in bond lengths, valence angles, and torsion structural parameters obtained after geometry optimization by both DFT methods can be noted in Table 1.

As for the isolated anionic moiety, a transformation from the Cartesian to the internal coordinate space allowed scaling of the internal force constants. A high general scaling factor of 0.98 was appropriate to fit most of the theoretical wavenumbers to the experimental vibrational data. Table 2 displays the potential energy distribution (PED) among internal coordinates corresponding to DFT calculations at the B3LYP/6-31++G** level.

A root-mean-square deviation (RMSD) of 17.4 cm^{-1} between the theoretical DFT and experimental vibrational frequencies was presently calculated when using only this single scaling factor.

In a first attempt, we did not try to determine specific scaling

TABLE 3: D-Glucuronic Acid Sodium Salt[a]

ν (cm^{-1})	assignments
76.9	0.66τC4O4 + 0.14τO5C5 + 0.11δO5C5C4 + 0.10τC4C5
112.3	0.30τC1O5 + 0.26δO5C5C6 + 0.15τC5C6 + 0.14δC1O5C5 + 0.14δC3C4C5
133.7	0.42τC5C6 + 0.25τC2C3 + 0.20τC3C4 + 0.11C3O3
158.6	0.59τC1O1 + 0.17τO2C2 + 0.13δC1C2C3 + 0.13δO5C1O1
221.9	0.93τC1O1 + 0.04τC2O2 + 0.02δO1C1C2
238.9	0.90τC1O1 + 0.09τC2O2
289.1	0.81τC2O2 + 0.11δO2C2C3 + 0.05τC3O3 + 0.03δO3C3C4
293.9	0.81τC2O2 + 0.07δO1C1C2 + 0.06τC1O1 + 0.06τC4O4
319.6	0.36δO2C2C3 + 0.22δC2C3O3 + 0.20δO5C1C2 + 0.11τC3O3 + 0.11τC2O2
327.9	0.64τC4O4 + 0.19δO5C1O1 + 0.11τO1C1 + 0.07τO2C2
336.2	0.82τC4O4 + 0.09δC1C2O2 + 0.05δO5C5C4 + 0.04δO5C1O1
352.0	0.51τC3O3 + 0.49τO4C4
380.5	0.72τC2O2 + 0.28τC4O4
397.3	0.21νC2C3 + 0.21νC1O1 + 0.19νO5C5 + 0.13νC4O4 + 0.13δC1O5C5 + 0.13τC4O4
425.9	0.34τC3O3 + 0.13τO2C2 + 0.09τC1O1 + 0.08δCTCTCT + 0.08δCTCTOH
435.6	0.73τC3O3 + 0.27τC4O4
450.0	0.56τC3O3 + 0.43τC4O4
467.1	0.43τC1O1 + 0.33τC2O2 + 0.13δO5C1C2 + 0.11δO4C4C5
518.8	0.33νC2O2 + 0.20δC1C2O2 + 0.18νO5C1 + 0.10δO5C1C2 + 0.10δ(CO2-) + 0.09δO5C1O1
535.2	0.34νC4C5 + 0.26δO4C4C5 + 0.12δO5C1O1 + 0.10δO3C3C4 + 0.09νC4O4 + 0.09νC3O3
608.7	0.30δC1O1 + 0.27δ(CCO) + 0.30δC1O1 + 0.16δO5C5C6 + 0.15δC2C3O3 + 0.13νO5C5
619.5	0.25δO2C2C3 + 0.22δC3C4O4 + 0.17δC2C3O3 + 0.14δ(CCO) + 0.14γ(CO2-) + 0.09δ(CO2-)
648.9	0.30νC1O1 + 0.24δC1O5C5 + 0.14νC5C6 + 0.14δ(CCO) + 0.10νC4O4 + 0.08δO5C_5C4
734.6	0.89γ(CO2-) +0.07δC4C5C6 +0.04δC3O3
906.6	0.36νC5C6 + 0.27νC1O1 + 0.13νO5C1 + 0.13ν(CO2-) + 0.08νO5C5 + 0.04δC1O5C5
959.0	0.35νC2C3 + 0.23νC3O3 + 0.15νC1C2 + 0.13νC2O2 + 0.10νC4O4 + 0.04νC4C5
979.6	0.30νC3C4 + 0.21νC3O3 + 0.19νC4O4 + 0.11νC4C5 + 0.10νO5C1 + 0.09νC2O2
999.6	0.57νC1C2 + 0.22νC2O2 + 0.06δC1C2O2 + 0.06νC2C3 + 0.05δC1H + 0.05νO5C1
1055.3	0.30νC4C5 + 0.20νC3O3 + 0.19νC4O4 + 0.16νO5C5 + 0.08νC1O1 + 0.07νC2C3
1061.8	0.51νO5C1 + 0.21νC3C4 + 0.10νO5C5 + 0.07νC1C2 + 0.06νC2O2 + 0.06δC1O1H
1069.3	0.30νC1O1 + 0.21νC4C5 + 0.20νC2O2 + 0.12νC1C2 + 0.12νO5C1 + 0.06νC3C4
1090.1	0.55νC4O4 + 0.16δC4C5HC + 0.13νC3C4 + 0.11νO5C5 + 0.05νC1C2
1129.4	0.34νC3O3 + 0.24νO5C5 + 0.18νC3C4 + 0.15νC2C3 + 0.04νC2O2 + 0.04νC5C6
1139.9	0.56νC2O2 + 0.20νC2C3 + 0.11νO5C1 + 0.05δC1O1H + 0.04νC3C4 + 0.04νC1C2
1162.5	0.27νC4O4 + 0.23νO5C5 + 0.20νC4C5 + 0.18νC3O3 + 0.06δC4H + 0.05νC6−O
1187.3	0.35δC1H + 0.23δC1O1H + 0.17νC1O1 + 0.15δC2H + 0.11νC3O3
1208.0	0.29νC1O1 + 0.22δC1H + 0.13νO5C5 + 0.12δC2H + 0.12δC1O5C5 + 0.11δC1O1H
1242.7	0.51δC1O1H + 0.20δC1H + 0.13δC1O5C5.08νO5C5 + 0.07δC2O2H
1264.9	0.55δHCC3C4 + 0.23δC2H + 0.13δC3O3H + 0.09δC4H
1302.2	0.61δC2O2H + 0.14δC1O1H + 0.12νs(CO2-) + 0.04νO5C1 + 0.04δC1H
1318.0	0.52νs(CO2-) + 0.17νC5C6 + 0.04δC3O3H + 0.03δC2O2H + 0.01δ(OCO)
1321.9	0.67δC3O3H + 0.12δC4H + 0.06νs(CO2-) + 0.05δC2O2H + 0.05νC3O3 + 0.05νC4O4
1338.2	0.33δO5C1HC + 0.23δC1O1H + 0.23νO5C1 +0.11δHCC3O3 + 0.10νC1O1
1362.6	0.46δC5H + 0.24δC4H + 0.20δC3O3H + 0.11νO5C5
1386.1	0.35δC2H + 0.26δC3H + 0.16νC2O2 + 0.12νC3O3 + 0.11νO5C1
1404.4	0.43δC5H + 0.25δC4H + 0.18νC4O4 + 0.15νO5C5
1408.5	0.23δC1O1 + 0.20νC1O1 + 0.17δC1H + 0.12νC1C2 + 0.09δC2H + 0.08δC1O5C5
1443.1	0.44δC3H + 0.34δHCC2 + 0.14νC2C3 + 0.08νC2O2
1449.4	0.90δC4O4H + 0.05νa(CO2-) + 0.05νCTCT
1543.3	0.61δC4H + 0.20νa(CO2-)
1587.9	0.91νa(CO2-)
2922.3	0.43νC3H + 0.24νC2H + 0.17νC4H + 0.10νC1H + 0.06νC5H
2927.3	039νC1H + 0.24νC5H + 0.20νC4H + 0.15νC2H
2933.4	0.38νC5H + 0.31νC3H + 0.27νC1H
2944.2	0.38νC2H + 0.24νC4H + 0.20νC5H + 0.17νC1H
2949.7	0.35νC4H + 0.23νC2H + 0.22νC3H + 0.13νC5H + 0.06νC1H
3504.7	0.62νO2H + 0.32νO1H + 0.06νO3H
3511.9	0.61νO1H + 0.21νO3H + 0.17νO2H
3513.5	0.72νO3H + 0.21νO2H
3547.5	1.00νO4H

[a] Vibrational wavenumbers (in cm^{-1}) and potential energy distribution among internal coordinates as obtained from the SPASIBA empirical force field. ν: stretching. ν_a and ν_s: antisymmetric and symmetric stretching modes. δ: in-plane valence bending. γ: out-of-plane wagging. τ: torsion.

factors attached to each internal coordinate type, this being principally due to the complexity of the normal modes. With this in mind, DFT calculations using only one general scaling factor offer an approximative general description of the vibrational potential energy distribution among internal coordinates. This could explain the rather large RMSD obtained between experimental data and theoretical wavenumber values.

No internal hydrogen bond could now be detected between the O4 hydroxyl hydrogen and a carboxylate oxygen atom as observed above for the isolated anionic form. The antisymmetric ν_a (CO2) mode is always predicted to occur in the 1580−1590 cm^{-1} range, while a considerable change occurs for the symmetric mode. This mode is now quite well predicted to occur between 1360 and 1400 cm^{-1}.

The out-of-plane wagging mode of the carboxylate group shows numerous contributions to several modes between 520

and 700 cm^{-1}. The δ(CCO) in-plane bending is rather well located in the 410−460 cm^{-1} range, while the corresponding in-plane bending δ(OCO) contribution appears near 800 cm^{-1}. One can note the large mixing of the in- and out-of-plane motions with the endocyclic νCC, νCO and δCCO5, δCCC vibrational motions with participation of bending modes of the exocyclic hydroxyl groups. The in-plane vibrations remain defined in the same wavenumber range than those obtained in the previous calculation with the 6-31G** basis set.

Different scaling values were applied to the γ(CO2) out-of-plane mode, but only small shifts in frequencies could be detected. This mode can then be considered as being "frozen" by the presence of the counterion.

The local group motions of the exocyclic δCH and δC−O groups are well-defined in the 1500−1200 cm^{-1} domain, and νC−OH motions occurring in the range 1200−1000 cm^{-1} have comparable corresponding wavenumbers and potential energy distribution among internal coordinates than those predicted for the pure anionic form. The 1000−600 cm^{-1} region corresponds to the δ(CCOH) and δ(CCO), δ(COC) ring-bending modes.

It can be easily observed that the use of diffuse functions and inclusion of a counterion only operate on the normal modes of the anionic part of the molecule. The present general scaling factor is close to unity for the major part of the internal force constants. In our mind, this offers a good example of the necessity to add a counterion and to use an adapted basis set including diffuse functions when dealing with charged species in quantum mechanical studies.

III.a.3. Normal-Mode Analysis Using the Empirical SPASIBA Force Field. As could be asserted from the former arguments, DFT calculations using adequate basis functions and addition of counterions can be of great help to obtain reliable vibrational assignments when no experimental assignments could be obtained.

The SPASIBA force field is a spectroscopically derived force field and was applied in previous normal-mode analyses on mono- and disaccharides by our group.[23,26] Here, we used the existing SPASIBA force constant database with very few modifications. Torsional potentials related to ring bonds and exocylic hydroxyl groups were deduced from spectroscopic data on crystal forms of monosaccharides and extended to a variety of glycosidic linkages appearing in disaccharides.[14,15]

Examination of the low-frequency region (76−300 cm^{-1}) reveals a good agreement with the DFT predictions, in particular, for the monosaccharide ring normal modes involving CT-CT, CT-O5, and exocyclic hydroxyl group torsional librations and ring deformations.

Comparison between the DFT and SPASIBA-derived geometry parameters (Table 1) leads to some important remarks regarding mainly the carboxylate group. The two C6−O bonds remain on the same order of length when using molecular mechanics but are predicted to have different values in both DFT calculations; this fact implies unequal electronic properties betwen the two bonds. The SPASIBA torsional C5−C6 equilibrium value displays a large difference (about 50°) from the corresponding ones obtained from DFT calculations. The corresponding SPASIBA torsional parameter was derived from vibrational analyses using pure C_{2v} symmetry which, in fact, does not seem to correspond presently to the case predicted by DFT methods.

Table 3 displays the potential energy distribution (PED) obtained for the D-glucuronate isolated anion. A RMSD of 34.5 cm^{-1} is obtained between the experimental and SPASIBA-derived vibrational wavenumbers. The largest discrepancies between molecular mechanics predictions and experimental data stand in the 510−540 and 620−740 cm^{-1} spectral ranges, both implying the participation of valence angles and out-of-plane motions attached to the carboxylate group. This is mainly responsible for the relative large deviations from experimental data.

TABLE 4: Geometry Parameters for D-Galactosamine 4-Sulfate as Derived from Theoretical DFT Calculations and the Empirical SPASIBA Force Field[a]

	DFT B3LYP /6-31G** (1)	DFT B3LYP /6-31++G** (2)	SPASIBA
C5−O5	1.440	1.442	1.442
C1−O5	1.426	1.396	1.430
C4−OT	1.423	1.422	1.477
OT−S	1.718	1.708	1.712
S−O	1.493[b]	1.490	1.465
	1.476	1.498	1.462
	1.465	1.461	1.463
C4−OT−S	115.7	118.9	115.9
OT−S−O	102.7[b]	99.8	105.2
	104.0	106.4	105.5
	101.3	103.1	104.9
O−S−O	114.2[b]	117.8	113.4
	115.0[b]	110.6	113.2
	116.7	116.5	113.5
C3,C4−OT,S	−98.8	−122.0	−113.3
C5,C4−OT,S	141.0	115.6	125.7
H1,C1−O1,HO	64.9	64.8	44.3
H3,C3−O3,HO	−148.0	65.5	−102.6
O5,C5−C6,O6	58.0	52.3	59.0
C4,C5−C6,O6	−179.1	173.5	−175.1
C1,C2−N,C	92.5	−153.9	97.3
C3,C2−N,C	−150.0	−34.3	−141.9
C2,N−C,CT	163.6	−173.0	−179.5
H,N−C,O	−156.9	175.9	179.2
HO3····O−S	1.71		2.02
O3,HO3····O−S	167.7		158.4
C3,O3−HO3····O−S	62.9		−78.5
O3,HO3····O−S	−50.6		42.1
HO3···O(C═O)		1.557	
HO3···O═C		115.6	
O3−HO3···O(C═O)		163.7	
O3−HO3···O═C		23.5	

[a] Distances are given in angstroms and bond valence angles in degrees. (1) isolated anionic form; (2) diffuse functions added in the presence of the Na^+ counterion. [b] Refer to the O atom displaying a hydrogen-bonded character with the C4 hydroxyl hydrogen.

On the contrary, the empirical force field constants associated with the carboxylate group, being deduced from experimental data assuming a C_{2v} symmetry type, lead to correct assignments of the antisymmetric stretching mode, which is well-reproduced at 1570−1600 cm^{-1}, while the corresponding symmetric mode is predicted to occur at about 1320 cm^{-1}.

Along empirical minimization without distance constraints of the D-glucuronate anion in the presence of its counterion primitively spreading in the OCO plane, the Na atom moves out of the OCO plane at a C−O distance of 3.47 Å from the O4 oxygen atom. A new strong contribution to the ν_s (CO2) mode is then calculated at 1361 cm^{-1}.

III.b. D-Galactosamine 4-Sulfate Sodium Salt. Due to the large instability at room temperature of the sodium salt form of D-galactosamine 4-sulfate, we did not achieve success in recording the infrared and/or Raman spectra. We shall thus use the IR linear dichroism data reports of Servaty et al.[1] on hyaluronic acid and chondroitin sulfate and IR measurements of Matsuhiro et al.[30] to support our theoretical predictions on some vibrational wavenumbers and assignments.

Two types of quantum mechanical treatments have been carried out in the present work.

TABLE 5: DFT/B3LYP Derived Vibrational Wavenumbers (in cm^{-1}) on D-Galactosamine 4-Sulfate in Its Isolated Anionic Form[a] and in the Presence of Its Sodium Counter Ion[b,c]

6-31G**[a]	6-31++G**[b]	potential energy distribution (in the presence of the sodium counterion)
48.5	63.0	0.62τCTCT + 0.18τCTN + 0.13τCN + 0.06τOT−S
58.1	78.6	0.29τCTO5 + 0.28τCTCT + 0.16δCT−N + 0.15γNH + 0.10τCN
99.5	86.9	0.38τOT−S + 0.32τCTCT + 0.12τCN + 0.09τCTN + 0.04γNH
55.1	105.5	0.81τC4−OT + 0.19τOT−S
	113.7	0.55τOT−S + 0.36τC5C6 + 0.08δC4−OT−S
99.5	114.9	0.36τOT−S + 0.18τC5C6 + 0.12δCTCTOT + 0.08δ(SO3) + 0.08τC1O1 + 0.006τC4OT + 0.06γNH
123.3	127.3	0.29τCTCT + 0.12τCN + 0.11δC5C6 + 0.11γNH + 0.11τCTN + 0.08τC5O5 + 0.06δCTCTCT
110.1	137.8	0.46τC−CT + 0.16δCT−N + 0.23δC5C6 + 0.15τCTCT
150.2	159.0	0.23τCN + 0.22τC−CT + 0.21γNH + 0.16τCTCT + 0.09δCTN
168.6	176.2	0.34τCTCT + 0.33τCT−O5 + 0.1δC1O5C5 + 0.10δC1O1 + 0.07δCT−OT + 0.06δC4OTS
190.4	188.7	0.36τCTO5 + 0.27δC5C6 + 0.21δCT−OT + 0.10δC1O5C5 + 0.07δC5C6O6
177.4	201.3	0.67δC4−OT−S + 0.20δ(OT−S−O) + 0.12τOT−S
214.3	214.4	0.25τCTCT + 0.21τCTO5 + 0.15τC5C6 + 0.11δC2O2 + 0.11δC5C6 + 0.09νOT−S
227.0	238.5	0.29τOT−S + 0.19τCTO5 + 0.18δC1O1 + 0.18δC5C6 + 0.11δ(O−S−O) + 0.10τOTCT + 0.08δC5C6O6
273.8	264.8	0.44δCT−N−C + 0.19δNH + 0.13δC═O + 0.09δC2O2 + 0.07δN−C−CT + 0.07τNC
273.8	295.5	0.26δCT−N + 0.21δN−C−CT + 0.15δCTCTO5 + 0.12δC═O + 0.10νCTCT + 0.08νC5C6 + 0.06νCTN
348.4	337.8	0.26δ(OT−S−O) + 0.25τCN + 0.18τCTO5 + 0.12δC3O3 + 0.11δCTCTCT + 0.06δ(O−S−O)
410.0	341.3	0.72τC1O1 + 0.15δC1O1 + 0.12τC−CT
361.4	364.5	0.40δ(OT−S−O) + 0.13δ(O−S−O) + 0.21τOT−S + 0.12δCT−OT + 0.08τC1O1 + 0.06τCT−OT
392.8	373.8	0.45δ(OT−S−O) + 0.12δ(O−S−O) + 0.12τC6O6 + 0.12δCTN + 0.10τC1O1 + 0.07δC5C6O6
429.5	396.6	0.31δC3O3 + 0.27τC6O6 + 0.20δCTOT + 0.16δ(OT−S−O) + 0.05δ(O−S−O)
410.0	398.5	0.31τC6O6 + 0.17τC1O1 + 0.11δCT−N + 0.05δC3O3
429.5	420.6	0.23τC−CT + 0.22δCTCTCT + 0.17νCTCT + 0.14δC1O1 + 0.12δCT−N + 0.09δCTCTO5
429.5	432.5	0.26δCTCTO5 + 0.21δC5C6O6 + 0.16τC6O6 + 0.14δNH + 0.11δ(O−S−O) + 0.10δCTO5CT
478.1	476.0	0.45δ(O−S−O) + 0.30νOT−S + 0.17δ(OT−S−O) + 0.07τCTCT
488.5	486.0	0.26δC═O + 0.20δCTOT + 0.15δCTC5C6 + 0.12δ(OT−S−O) + 0.09νOT−S + 0.09δCTN + 0.07δ(O−S−O)
519.1	510.4	0.47δ(O−S−O) + 0.18δC1O1 + 0.15δCTOT + 0.11δ(OT−S−O) + 0.09νCT−OT
534.2	534.5	0.38δC3O3 + 0.25δC1O1 + 0.14δC═O + 0.13δC5C6 + 0.09δC5C6O6
520.5	541.5	0.81δ(O−S−O) + 0.19δ(OT−S−O)
561.2	552.3	0.41δ(O−S−O) + 0.34δ(OT−S−O) + 0.13δ(CT−OT−S) + 0.11τOT−S
581.7	579.7	0.30δC═O + 0.21δC1O1 + 0.18δC1H + 0.16δC5C6 + 0.14γC═O
609.6	586.6	0.77γC═O + 0.23γNH
621.8	607.8	0.26δ(CT−OT−S) + 0.22νOT−S + 0.20δC═O + 0.14δ(O−S−O) + 0.10δC3O3 + 0.08νC−CT
656.2	669.0	0.27δC4−OT + 0.22νOT−S + 0.16δCTCTO5 + 0.13δC3H + 0.08δC═O + 0.07νN−CT + 0.06τCTN
	679.3	0.37τCN + 0.34τCTN + 0.15γC═O + 0.14γNH
699.5	700.3	0.46δC4−OT + 0.33δC═O + 0.20νCTCT
812.5	789.5	0.22δCTCTO5 + 0.16δC4H + 0.15δC4−OT + 0.15νOT−S + 0.15νCTCT + 0.11νCTN + 0.05νC4OT
864.8	859.3	0.32νC5O5 + 0.16ρCH2 + 0.14δC1O5C5 + 0.11δC1O1 + 0.09νCTCT + 0.09νC5C6 + 0.08δCTCTCT
875.8	868.6	0.38νC4−OT + 0.16νCTCT + 0.11δC3H + 0.10δCTN + 0.09νC−CT + 0.08νCN + 0.08νOT−S
691.3	893.3	0.99τC3O3
917.6	907.2	0.30ρCH2 + 0.24τC3O3 + 0.18νC5C6 + 0.14νC4−OT + 0.07δC5H + 0.06νCN
917.6	936.9	0.58τCTCT + 0.12ρCH2 + 0.10νCN + 0.09δC5H + 0.06δC1H + 0.05δCTCTCT
956.6	951.6	1.0ν(SO3)
1010.6	979.5	0.38ρCH2 + 0.21νC−CT + 0.13νCTN + 0.1νCTCT + 0.06νC3O3 + 0.05νC5C6 + 0.04νC4−OT
1010.6	1001.4	0.35ρCH2 + 0.17νC5C6 + 0.15νCTCT + 0.13νC6O6 + 0.11νC4−OT + 08νCT−O5
1001.8	1018.2	0.34νCTCT + 0.21νC3O3 + 0.16νC1O1 + 0.11νC−CT + 0.10δC═O + 0.07δC1O1H
974.4	1030.0	0.81ρCH3 + 0.19γC═O
1010.6	1033.6	0.68νC6O6 + 0.17νC5C6 + 0.14ρCH2
1097.3	1041.8	0.35νC3O3 + 0.21νC6O6 + 0.12δC1O1H + 0.11νC1O1 + 0.10δC3H + 0.09δC2H
1119.6	1057.8	0.21νCTN + 0.18νC1O5 + 0.16δCTCTCT + 0.15νCTCT + 0.12νC5C6 + 0.08ρCH3 + 0.08νC3O3
1087.0	1070.5	0.34ρCH2 + 0.31νC6O6 + 0.18νCTO5 + 0.08νC5C6 + 0.08δC6O6H
	1084.6	0.30ρCH2 + 0.27νC6O6 + 0.21νCTN + 0.15νCTCT + 0.06δC6O6H
1097.3	1096.1	0.39νC1O5 + 0.25νC4OT + 0.18νCTN + 0.17δCTCTCT
1060.1	1120.1	0.76νCTO5 + 0.14νCTCT + 0.09νC4−OT
1148.6	1123.1	1.0ν(SO3)
1163.4	1126.4	0.55νC1O1 + 0.20ν(SO3) + 0.17νC3O3 + 0.06δCTCTCT
1204.2	1197.9	0.36twiCH2 + 0.21δC6O6H + 0.15δC2H + 0.15δC1H + 0.12δC1O1H
1221.8	1215.5	0.29twiCH2 + 0.25δC1H + 0.19δC2H + 0.17δC6O6H + 0.09δC1O1H
1258.3	1244.6	0.32δC5H + 0.30δC4H + 0.27ν(SO3) + 0.11δC1H
1232.3	1247.7	0.68ν(SO3) + 0.18δC1O1H + 0.13δC1H
1251.1	1249.1	0.28ν(SO3) + 0.19δC1O1H + 0.19δC4H + 0.12δC5H + 0.10δC1H + 0.10δC2H
1258.3	1265.4	0.51δC2H + 0.39δC3H + 0.10νCN
1303.7	1290.7	0.46δC3H + 0.22νCN + 0.18δNH + 0.07νCT−N + 0.06νC−CT
1258.3	1296.6	0.32δC4H + 0.31δC5H + 0.14δC3H + 0.14waγCH2 + 0.07νCTCT
1317.3	1306.4	0.37δC5H + 0.33δC1O1 + 0.30δC2H
1341.5	1327.7	0.32δC5H + 0.30δC2H + 0.15δC1H + 0.15δC4H + 0.08δC3H
1341.5	1347.6	0.55δC4H + 0.35δC3H + 0.10δC1H

TABLE 5: Continued

6-31G**[a]	6-31++G**[b]	potential energy distribution (in the presence of the sodium counterion)	6-31G**[a]	6-31++G**[b]	potential energy distribution (in the presence of the sodium counterion)
1353.3	1352.6	0.47wagCH2 + 0.42δC6O6H + 0.10δC3H	2904.5	2888.3	0.81νC5−H + 0.19νC3−H
1365.9	1362.1	0.42δC4H + 0.37δC3H + 0.10δC2H + 0.10δC5H	2881.6	2900.2	0.81νC3−H + 0.19νC5−H
1370.1	1372.2	1.0δsCH3	2921.6	2906.2	1.0νsCH3
1383.0	1374.7	0.65δC1H + 0.29δC5H + 0.06δC6O6H	2947.6	2933.1	1.0νsCH2
1407.7	1391.6	0.82wagCH2 + 0.10δC6O6H + 0.07δC5H	3043.6	2973.5	1.0νC2−H
1435.5	1407.4	0.65δC1H + 0.21δC1O1H + 0.08δC2H + 0.06νCTCT	2988.9	2977.3	1.0νaCH3
1448.2	1433.4	1.0δaCH3	2984.6	2979.0	1.0νC4−H
1464.0	1449.7	1.0δaCH3	3002.0	2985.8	1.0νaCH2
1481.6	1459.2	1.0sciCH2	3010.3	2987.0	1.0νaCH3
1472.0	1510.4	1.0δC4O4H	3241.0	3296.0	1.0νO3−H
1509.7	1528.0	0.67δNH + 0.32νCN	3520.9	3461.0	1.0νN-H
1644.6	1648.4	0.82νC═O + 0.09δNH + 0.09νCN	3702.3	3664.7	1.0νO1−H
2839.9	2837.4	1.0νC1−H	3695.7	3681.2	1.0νO6−H

[c] ν: stretching. δ: in-plane bending. τ: torsion. γ: out-of-plane wagging. ρ: rocking mode for methyl and methylene groups. ν_a, ν_s: antisymmetric and symmetic stretching modes. δ_a, δ_s: in-plane bending antisymmetric and symmetric modes. Force constants scaling factors: 0.95 for the C−H stretching modes of the CH2 and CH3 groups, 1.00 for the O3−H stretching mode, and 0.97 for all others.

(i) The D-galactosamine 4-sulfate moiety was first investigated in the isolated anionic form. The related optimized DFT/B3LYP/6-31G** geometry displays a chair conformation, and one can note the presence of a hydrogen-bond-like structure between the HO3 hydrogen atom and an oxygen atom of the SO3 group. The amide hydrogen atom spreads toward this last atom with, however, no hydrogen bond setting up. Table 4 displays the current structural values obtained from DFT optimizations for this structure.

(ii) The second molecular model includes a Na^+ counterion placed primitively as a bidentate structure in the OSO plane neighboring the O3 hydroxyl oxygen atom. The geometry optimization was performed via the DFT/B3LYP/6-31++G** method implying diffuse functions to take into account the particular electronic effects related to the anionic structure. After geometry optimization, the bidentate structure displays a mean $Na^+\cdots O$ (SO3) distance of 2.34 Å, while the sugar ring is still in a chair conformation. The carbonyl oxgen atom of the acetyl amide group lying at the C2 ring position undergoes one hydrogen bond with the hydroxyl hydrogen of the hydroxyl O3 group. Such a hydrogen bond changes the relative orientation of the C3O3H hydroxyl group (65.5°), which is to compare to the calculated DFT dihedral angle (−148°) when no internal hydrogen bond exists (Table 4). The DFT-optimized C2−N torsional parameter is predicted to take very different values when a Na^+ counterion (and hydrogen bond) is present (−154°, −34°) or not (92°, −150°).

The sulfate group displays an approximate C_{3v} geometry, while the exocyclic hydroxyl groups display gauche conformations (at C1 and C3) and a gauche−trans conformation for the hydroxymethylene group as can be also noted in the isolated anionic form.

The potential energy distribution among internal coordinates and theoretical wavenumbers have both been deduced from DFT calculations using the force constant scaling method of Allouche et al.[11] A general scaling factor of 0.98 was used for the isolated anion, and a corresponding factor of 0.97 for the bidentate complex. Only a few scaling factors have to be modified to fit the experimental data (see footnotes in Table 5).

III.b.1. DFT-Derived Normal Modes Implying the Sulfate Group. Table 5 displays the DFT vibrational wavenumbers obtained at the B3LYP/6-31G** level for the isolated anionic form of this compound and the corresponding ones for the bidentate complex using diffuse functions and its associated counterion (B3LYP/6-31++G**).

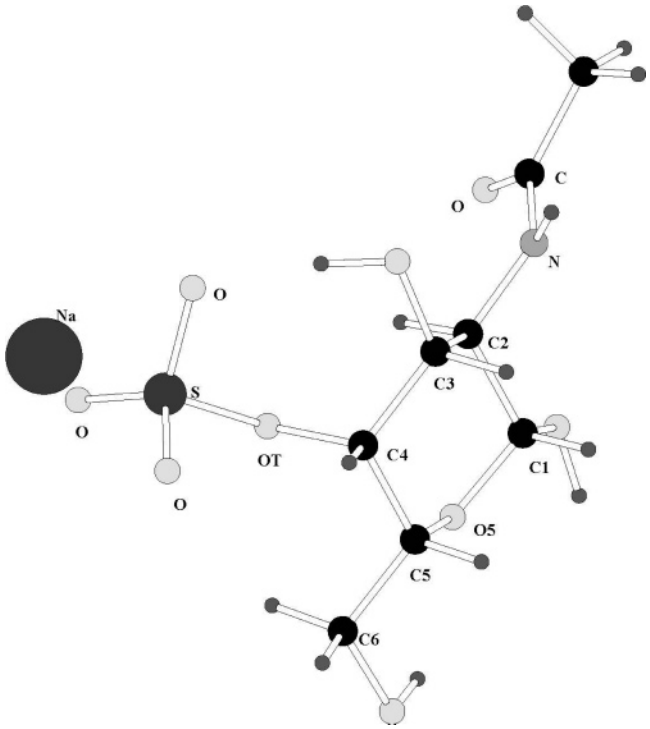

Figure 2. D-Galactosamine 4-sulfate sodium salt (ball-and-stick representation).

Matsuhiro[30] attributed a band observed at 1261 cm^{-1} to a νS═O-type vibration, while Servaty reported two bands at 1226 and 1063 cm^{-1} as originating from the ν_{as} antisymmetric stretching modes of the $SO3^-$ group.[1] From examination of the internal parameters obtained after geometry optimization (Table 4), one can observe that one of the S−O bonds is longer than the other two in the isolated anionic form of D-galactosamine 4-sulfate, as it undergoes formation of an internal hydrogen bond between the oxygen and the hydrogen O4 hydroxyl atom (Figure 2). We will assume here a pratically regular tetrahedral conformation for the charged $OSO3^-$ moiety, as we obtained the two corresponding ν_{as} (SO3) modes at 1233 and 1148 cm^{-1} for the isolated anionic form and at 1247 and 1123 cm^{-1} for the bidentate complex. Boggs et al.[31] identified this mode to occur in the 1216−1223 cm^{-1} range using FTIR measurements on sulfate cerebroside (CBS) and could observe only very small frequency changes upon Ca^{2+} complexation.

TABLE 6: Calculated Wavenumbers and Potential Energy Distribution of D-Galactosamine 4-Sulfate as Obtained from the Empirical SPASIBA Force Field[a]

ν (cm^{-1})	assignments
36.3	0.60τC1O1 + 0.30τC3O3 + 0.10τC2N
38.3	0.74τOT-S + 0.15τC1O1 + 0.08τC3O3
46.4	1.0τC1O1
55.6	0.95τC1O1
67.5	0.96τC1O1
70.4	0.90τC1O1 + 0.06τC3O3
81.7	0.90τC−CT + 0.08τC1O1
82.0	0.73C1O1 + 0.15τC−CT + 0.12τCN
102.6	0.61τC5C6 + 0.32C1O1 + 0.06τC6O6
140.5	0.96τC3O3
158.7	0.55τC3O3 + 0.45τC6O6
164.3	0.98τC3O3
183.0	0.65τC3O3 + 0.15τC6O6 + 0.10δCTNC + 0.09δCTCTCT
195.4	0.70τC3O3 + 0.22δCT−OT−S + 0.08δOT−S−O
218.4	0.34δC3C4OT + 0.18δOT−S−O + 0.18τC1O5 + 0.17νC4OT + 0.13νOT−S
231.0	0.30δO5C5C4 + 0.21δOTC4C5 + 0.16δC1O5C5 + 0.11δOT−S−O + 0.11νC3C4 + 0.11τO5C5
243.6	0.37τC1O1 + 0.31δC1O1 + 0.23δO5C5C6 + 0.10τC6O6
252.7	0.23δOTC4C5 + 0.22νC2N + 0.15δC5C6O6 + 0.14δC3O3 + 0.14νNC + 0.12δO5C1C2
292.8	0.42δC1O1 + 0.20δC3O3 + 0.15νC4C5 + 0.12νC3C4 + 0.11νC1C2
296.8	0.60τCN + 0.14δCTN + 0.09γC=O + 0.09δC3O3 + 0.06τC3O3
348.7	0.26δC5C6O6 + 0.24δC1O1 + 0.15δC3O3 + 0.13νC4C5 + 0.10δCTN + 0.10νC3O3
381.0	0.37δ(OT−S−O) + 0.20δCTCTO5 + 0.20νCTOT + 0.17δC=O + 0.05νOT−S
426.6	0.32δ(OT−S−O) + 0.25δ(O−S−O) + 0.15νC3O3 + 0.15νCTCT + 0.11δCTCTCT
450.0	0.36δ(OT−S−O) + 0.20δC1O1 + 0.14νC1O1 + 0.10δCTCTCT + 0.09νC3O3 + 0.09νO5CT
480.0	0.43δ(OT−S−O) + 0.18δ(O−S−O) + 0.14δCTCTO5 + 0.12νC1O1 + 0.11νOT−S
500.1	0.39δ(OT−S−O) + 0.14δCTO5CT + 0.14νC1O1 + 0.10δC3O3 + 0.08νC1O5 + 0.08νC5C6
513.2	0.53δ(OT−S−O) + 0.22δ(O−S−O) + 0.08δC=O + 0.08νC1O5 + 0.06δNCCT
524.9	0.82δ(O−S−O) + 0.10δ(OT−S−O) + 0.07νOT−S
541.7	0.76δ(O−S−O) + 0.14νS−O + 0.05δ(OT−S−O) δa(SO3)
545.7	0.77δ(O−S−O) + 0.14νS−O + 0.08δ(OT−S−O) δa(SO3)
561.9	0.26δC3O3 + 0.24γC=O + 0.24δC1O1 + 0.15δ(O−S−O) + 0.11δ(OT−S−O)
580.4	0.56γC=O + 0.39τNC
600.9	0.25δC1O5C5 + 0.17νC5C6 + 0.16δOTSOOS + 0.15δO5C1O1 + 0.13δO5C5C6 + 0.13νO5C5
623.5	0.48δC=O + 0.35νCCT + 0.08νNCT + 0.08δNH
664.7	0.46δCTCTOT + 0.18δC3O3 + 0.12δ(OT−S−O) + 0.10νC6O6 + 0.07δC5C6O6 + 0.07νC3O3
704.5	0.32τNC + 0.17νC4OT + 0.13γNH + 0.09δCTCTCT + 0.07νOT−S + 0.07δO5C5C4 + 0.06γC=O
759.7	0.50τNC + 0.30γNH + 0.12γC=O
878.0	0.28νO5C5 + 0.25ρCH2 + 0.21νCTCT + 0.16νC1O1 + 0.09νCN
882.0	0.37νS−O + 0.23νOT−S + 0.18νC4OT + 0.10νCCT + 0.06δCT−OT−S + 0.04νNC
902.6	0.55νS−O + 0.19νOT−S + 0.11νCCT + 0.08νNC + 0.06νC=O νs(SO3)
932.7	0.38νC4OT + 0.40νS−O + 0.11νNC + 0.10νC=O
944.0	0.82ρCH3 + 0.08νC=O + 0.05νNC + 0.04νCCT
963.9	0.48νC1C2 + 0.18νC1O1 + 0.13νC3O3 + 0.08νO5C1 + 0.07νC5C6 + 0.07δC1O1H
977.6	0.47ρCH3 + 0.35γC=O + 0.12τNC + 0.05γNH
984.4	0.30νC3O3 + 0.23νC4C5 + 0.22νC3C4 + 0.09νC1C2 + 0.09νC2C3 + 0.07νO5C5
1036.4	0.66νC6O6 + 0.09νC4C5 + 0.09νC3C4 + 0.06νC2C3 + 0.06νC1C2 + 0.05νC1O1
1039.9	0.30νC4OT + 0.23νC1C2 + 0.17νC1O1 + 0.11νC6O6 + 0.11νC2C3 + 0.08νO5C1
1065.3	0.28νC1O5 + 0.25νC2C3 + 0.20νC3C4 + 0.14νC4C5 + 0.06νC5O5 + 0.05δC3O3H
1069.7	0.28νO5C1 + 0.27νC6O6 + 0.17νC5C6 + 0.12νC4C5 + 0.08νC4OT + 0.08νOT−S
1091.0	0.41νOT−S + 0.22νS−O + 0.14νC3OH + 0.09νO5C5
1099.0	0.39νC3O3 + 0.31νOT−S + 0.08νC3C4 + 0.08νC4−OT + 0.10νS−O
1113.5	0.37νC1O1 + 0.35νO5C1 + 0.10νC4C5 + 0.07νC1C2 + 0.06νC5C6 + 0.06νC2N
1154.1	0.38νO5C5 + 0.16νC5C6 + 0.15νC4C5 + 0.14νC3OH + 0.09δC6O6H + 0.09νC4OT
1173.1	0.59νC2N + 0.14δC1O1H + 0.10νCCT + 0.08νNC + 0.05νC2C3 + 0.04δC2H
1210.8	0.42δC1O1H + 0.26δC6O6H + 0.20δC1H + 0.12δC1O5C5
1216.9	0.37δC6O6H + 0.19νC5C6 + 0.16νC1OH + 0.13δC1O5C5 + 0.09νC2N + 0.07νNC
1220.5	0.96νS−O + 0.02δO−S−O νa(SO3)
1225.5	0.86νS−O + 0.07δC6O6H + 0.04δC1O1H νa(SO3)
1226.9	0.62δC6O6H + 0.16δC5H + 0.10νO5C1 + 0.07δC1O5C5 + 0.06δC1O1H
1245.9	0.61δC3O3H + 0.16δC3H + 0.11δC1O1H + 0.07δC1H + 0.06νC3OH
1262.2	0.35δC1H + 0.29 νCN + 0.17νC−CT + 0.δC1O1H
1275.3	0.53δC3O3H + 0.34δC4H + 0.23νC3C4
1281.9	0.39twiCH2 + 0.18δC6O6H + 0.16δC4H + 0.11νO5C1 + 0.11δC1O1H
1293.9	0.33twiCH2 + 0.20δC1O1H + 0.20δC1H + 0.13νO5C1 + 0.12νC1O1
1296.2	0.86twiCH2 + 0.07δC1O1H + 0.07δC2C1O5
1309.2	0.70δC2H + 0.19δC3O3H + 0.10δC4H
1323.8	0.45δsCH3 + 0.14δC1H + 0.10νC2N + 0.09νO5C1

TABLE 6: Continued

ν (cm^{-1})	assignments
1330.9	0.54δsCH3 + 0.15νNC + 0.11νC2N
1344.3	0.38δC1H + 0.25δC3H + 0.23δC3O3H + 0.12δC5H
1363.5	0.64δC3H + 0.14νC3O3 + 0.12δC4H + 0.09νC3C4
1379.7	0.38δC1H + 0.18δC3H + 0.18δC4H + 0.10νC1O1 + 0.07νC1C2 + 0.07νC2N
1396.7	0.31νO5C5 + 0.31δC4H + 0.17δC5H + 0.10νC1O1 + 0.10δC1O1
1424.3	0.37δC5H + 0.22δC4H + 0.19δaCH3 + 0.11νC1O1 + 0.08wagCH2
1427.2	0.97δaCH3
1437.0	0.97δaCH3
1444.9	0.75 δC2H + 0.11δNH + 0.10δCT−N + 0.04νC═O
1455.8	0.95sciCH2
1541.1	0.45δNH + 0.22νCN + 0.16νC2N + 0.09νC═O
1648.8	0.80νCO + 0.10δNH + 0.07νCN
2873.1	1.0νsCH2
2903.4	1.0νaCH2
2914.6	1.0νsCH3
2970.2	1.00νC5H
2972.6	1.0νaCH3
2975.3	1.0νaCH3
2983.7	0.52νC2H + 0.25νC1H + 0.22νC3H
2990.8	0.98νC4H
2995.5	0.51νC3H + 0.47νC1H
3006.4	0.47νC2H + 0.27νC3H + 0.26νC1H
3445.1	1.00νNH
3681.1	1.0νO1H
3681.2	1.0νO6H
3688.8	1.0νO3H

[a] ν: stretching. δ: in-plane bending. τ: torsion. γ: out-of-plane wagging. ρ: rocking. ν_s, ν_a: symmetric and antisymmetric stretching modes. δ_s, δ_a: symmetric and antisymmetric in-plane bending modes.

The νC−O−S stretching modes of the sulfate groups have been identified by Grant et al.[32] using IR studies on heparins to occur in the 750−950 cm^{-1} range. According to these authors, the 890 and 937 cm^{-1} bands have to be related to C−O−S and ring deformations. The present work predicts the occurrence of ν(S−O) stretching modes at 956 and 961 cm^{-1} for the isolated anionic form and only one band at 952 cm^{-1} for the bidentate complex. A strong contribution to the νC4−OT vibrational mode is reported here at 869 cm^{-1} for the bidentate complex, while a corresponding νOT−S vibrational mode is obtained at 917 cm^{-1} for the isolated anionic form.

In-plane bending deformations involving the sulfate group, δ(OT−S−O) and δ(O−S−O) vibrations are predicted to occur in two distinct regions (340−520 cm^{-1}) and (480−560 cm^{-1}) for both models of D-galactosamine 4-sulfate. The number of DFT-derived normal modes devoted to the bending deformations of the O−SO3 group, however, does not correspond to the number expected for a C_{3v} symmetry when their numerous participations to the potential energy distribution (i.e., 622, 561, 520, 410, 393, 361, and 348 cm^{-1} for the isolated anionic form and 552, 541, 510, 476, 374, 364, and 338 cm^{-1} for the bidentate complex) are considered.

III.b.2. Hydroxyl Groups and Ring Modes. The hydroxymethylene group adopts a gt orientation in both calculations, while the C1 and C3 hydroxyl group have gauche (g, g′) orientations in the bidentate complex and approximatively gauche−trans (t−g) conformations in the isolated anionic form, with this trans form being related to the presence of the hydrogen-bond-like structure involving the O3H hydroxyl group.

In the 1500−1200 cm^{-1} range, most of the vibrational modes are due to the δCH and δCT−OH groups for both types of structures. This is in agreement with corresponding normal modes found for the D-glucuronic acid sodium salt. The 1200−1000 cm^{-1} region reflects principally the internal ring νCTCT, νCT-O5, and exocyclic stretching modes for both the isolated anionic and bidentate conformations. The 1000−600 cm^{-1} range implies in both cases the participation of the hemiacetal moiety, involving particularly endocyclic stretching and bending modes.

III.b.3. Empirically Determined Vibrational Frequencies Using the SPASIBA Force Field. A few empirical force constants, particularly those devoted to the sulfate group, had to be adapted to fit the DFT-predicted wavenumbers. Table 6 displays the calculated wavenumbers and related assignments for D-galactosamine 4-sulfate. The SPASIBA-derived potential energy distribution gives coherent results for ring and exocyclic hydroxyl group motions when compared to the present DFT predictions or to previous empirical calculations on sugars. A RMSD of 36.3 cm^{-1} is obtained here between the SPASIBA- and DFT-derived wavenumbers (as no experimental data are available) when using diffuse functions in the presence of the Na^+ counterion. As for D-glucuronic acid sodium salt, the DFT calculations were performed using only one general scaling factor. Further work has to be done to obtain a complete set of DFT-derived scaling factors corresponding to each type of internal coordinates leading to a better empirical force field determination.

In the present work, the same set of parameters (as obtained for D-glucuronic acid sodium salt) related to the ring CT−CT, CT−O5 torsional librations was used. For the sulfate group, the torsional motions appear less well localized than they are from DFT predictions; however, the optimized torsional CT−OT parameter agrees fairly well with the DFT value when using diffuse functions.

Moreover, the largest deviations between wavenumbers would originate principally from normal modes involving the in-plane bending δ(OT−S−O) and δ(O−S−O) motions leading to an increase of the RMSD values obtained between the DFT and empirical methods. The OTSO3 group stretching vibrations are predicted to occur in the 381−513 cm^{-1} range (with contribution of δ(OT−S−O) vibrational motions) and in the 524−546 cm^{-1} range for motions involving mainly the participation of the δ-(O−S−O) bending modes. Both regions remain, however, in

TABLE 7: SPASIBA Parameters Related to the Internal Coordinates of D-Glucuronic and D-Galactosamine 4-Sulfate Sodium Salts[a]

bond	K (kcal mol^{-1} Å^{-2})	R_0 (Å)
CT−CT	165.0	1.53
CT−HC	320.0	1.10
CT−C6	160.6	1.506
CT−C9	165.0	1.53
C9−HM	291.3	1.11
CT−O5	255.0	1.426
CT−OH	263.0	1.43
OH−HO	486.0	0.95
C−O(CO2$^-$)	515.0	1.24
C−N	365.2	1.32
N−H	439.0	1.00
C═O	615.0	1.236
C−CT	160.65	1.506
S−O	550.0	1.465
OT−S	400.0	1.712

valence angle	H (kcal mol^{-1} rad^{-2})	Θ_0 (deg)	F (kcal mol^{-1} Å^{-2})
CT−CT−CT	18.70	111.8	47.47
CT−CT−OH	26.40	109.2	50.0
CT−O5−CT	85.0	112.8	70.0
CT−CT−O5	21.0	110.0	55.0
O5−CT−OH	28.45	108.0	41.0
O5−CT−HC	16.0	109.3	60.1
HC−CT−OH	15.0	107.2	80.0
CT−N−H	17.23	114.5	51.0
CT−N−C	26.25	119.0	40.28
C−N−H	25.15	119.5	66.18
N−C−CT	9.0	100.8	57.54
N−C═O	36.0	123.0	115.10
CT−C═O	14.0	123.6	35.0
CT−OH−HO	28.40	108.2	41.40
HC−CT−HC	29.6	108.5	10.07
OH−CT−HC	20.55	109.5	50.0
C−CT−HC	11.65	109.5	73.37
O−S−O	55.0	112.2	10.0
OT−S−O	50.0	104.0	10.0
CT−CT−HC	15.89	109.5	69.43
N−CT−HC	20.85	109.5	69.05

torsion	$Vn/2$ (kcal mol^{-1})	n	γ
X−CT−CT−X	0.15	3	0
X−CT−O5−X	0.20	3	0
X−CT−OT−X	0.01	3	0
X−CT−C−X	0.25	2	180
X−OT−SO−X	0.20	3	0
X−CT−N−X	0.015	3	0
X−CT−O5−X	0.2	3	0
X−C−N−X	8.65	2	180
X−CT−OH−X	0.05	−3	0
	0.02	−2	0
	0.70	1	0

improper	$Vn/2$ (kcal mol^{-1})	n	γ
CT−N−C═O	11.0	2	180
CT−N−C−H	1.85	2	180
O−CT−C−O	11.0	2	180

[a] The specific Urey−Bradley−Shimanouchi force constants Kappa, LCH2, and trans-gauche used in this work originate directly from ref 13 and were not given here. R_0: equilibrium distance. θ_0: equilibrium value of the valence angle bending. Vn: torsional barrier. n: order. γ: phase.

accordance with the DFT predictions, spreading over the 348−478 cm^{-1} and 519−562 cm^{-1} ranges for the isolated anionic form on one hand and the 338−374 cm^{-1} and 476−552 cm^{-1} ranges predicted for the sodium salt form on the other hand. The empirically derived stretching νS−O modes show contributions at 882, 903, and 933 cm^{-1} and at 1220 and 1225 cm^{-1}. These values have to be related to the 956, 960, 1148, and 1232 cm^{-1} DFT values obtained for the isolated anionic form and to the 952, 1247, and 1249 cm^{-1} values obtained in the presence of the sodium counterion using diffuse functions in the basis set.

The in-plane δC═O and out-of-plane γC═O modes originating from the acetamide group have been predicted to occur in the 570−600 cm^{-1} range by both DFT and empirical methods. The amide II vibration obtained from the SPASIBA force field at 1548 cm^{-1} is in agreement with the DFT values (1510 and 1528 cm^{-1}). The amide I (νC═O) stretching mode is predicted at 1649 cm^{-1} (SPASIBA) and at 1644 or 1648 cm^{-1} (DFT). The out-of-plane bending vibration of the NH group (amide V) is in the present case badly defined by both DFT methods (760 cm^{-1} for SPASIBA).

The final empirical set of SPASIBA parameters deduced from the vibrational analysis are displayed in Table 7 and would have to be considered as a starting database for further molecular dynamics studies.

As no experimental vibrational data could be obtained for D-galactosamine 4-sulfate, it appears difficult to compare theoretical methods between them in more expanded detail.

Conclusion

In the present work, empirical parameters were obtained from DFT calculations performed on the two constituents of chondroitin sulfate, i.e., D-glucuronic acid and D-galactosamine 4-sulfate. For D-glucuronate, it has been shown that a sodium counterion and basis sets with diffuse functions along DFT calculations are necessary to correctly fit the CO2 group stretching vibrations to the experimental data. For D-galactosamine 4-sulfate, the use of diffuse functions and introduction of the counterion does not show such a marked effect. An empirical set of force constants has been obtained after comparison of DFT and experimental data when available, which will be used for further dynamical studies on copolymers of these two residues.

Acknowledgment. The authors thank the Centre de Ressources Informatiques de Haute-Normandie (CRIHAN) located at Saint-Etienne du Rouvray (France) for their support with the IBM-1600 cluster through the contract CPER 2000-2006.

Supporting Information Available: Two files containing data obtained with *Jaguar* 4.0 program. This material is available free of charge via the Internet at http://pubs.acs.org.

References and Notes

(1) Servaty, R.; Schiller, J.; Binder, H.; Arnold, K. *Int. J. Biol. Macromol.* **2001**, *28*, 121.
(2) Kaufmann, J.; Möhle, K.; Hofmann, H. J.; Arnold, K. *Carbohydr. Res.* **1999**, *318*, 1.
(3) Rodriguez-Carvajal, M. A.; Imberty, A.; Perez, S. *Biopolymers* **2003**, *69*, 15.
(4) Winter, W. T.; Arnott, S.; Isaac, D. H.; Atkins, E. D. T. *J. Mol. Biol.* **1978**, *125*, 1.
(5) Cael, J. J.; Winter, W. T.; Arnott, S. *J. Mol. Biol.* **1978**, *125*, 21.
(6) Millane, R. P.; Mitra, A. K.; Arnott, S. *J. Mol. Biol.* **1983**, *169*, 903.
(7) Scott, J. E.; Chen, Y.; Brass, A. *Eur. J. Biochem.* **1992**, *209*, 675.
(8) Zsiska, M.; Meyer, B. *Carbohydr. Res.* **1993**, *243*, 225.
(9) Scott, J. E.; Cummings, C.; Brass, A.; Chen, Y. *Biochem. J.* **1991**, *274*, 699.
(10) *Jaguar Program*, v 4.0; Schröndinger, Inc.: Portland, OR, 1999.
(11) *Redong Program*. Allouche, A.; Pourcin. B. *Spectrochim. Acta* **1993**, *49A*, 571.
(12) Pulay, P. *J. Mol. Struct.* **1995**, *347*, 293.
(13) Derreumaux, P.; Vergoten, G. *J. Chem. Phys.* **1995**, *102* (21), 8586.
(14) Vergoten, G.; Mazur, I.; Lagant, P.; Michalski, J. C.; Zanetta, J. P. *Biochimie* **2003**, *85*, 65.

(15) Lagant, P.; Nolde, D.; Stote, R.; Vergoten, G.; Karplus, M. *J. Phys. Chem. A* **2004**, *108*, 4019.

(16) Tristram, F.; Durier, V.; Vergoten, G. *J. Mol. Struct.* **1996**, *377*, 47.

(17) Chhiba, M.; Tristram, F.; Vergoten, G. *J. Mol. Struct.* **1994**, *326*, 35.

(18) Derreumaux, P.; Lagant, P.; Vergoten, G. *J. Mol. Struct.* **1993**, *295*, 203.

(19) Tristram, F.; Durier, V.; Vergoten, G. *J. Mol. Struct.* **1996**, *378*, 249.

(20) Zanoun, A.; Durier, V.; Belaidi, A.; Vergoten, G. *J. Mol. Struct.* **1999**, *476*, 261.

(21) Vergoten, G.; Fleury, G.; Tasumi, M.; Shimanouchi, T. *Chem. Phys. Lett.* **1973**, *19*, 191.

(22) Takeuchi, H.; Shimanouchi, T.; Tasumi, M.; Vergoten, G.; Fleury, G. *Chem. Phys. Lett.* **1974**, *28*, 449.

(23) Dauchez, M.; Derreumaux, P.; Vergoten, G. *J. Comput. Chem.* **1992**, *14* (3), 263.

(24) Durier, V.; Tristram, F.; Vergoten, G. *THEOCHEM* **1999**, *395*, 81.

(25) Dauchez, M.; Lagant, P.; Derreumaux, P.; Vergoten, G.; Sekkal, M.; Sombret, B. *Spectrochim. Acta* **1994**, *50A* (1), 105.

(26) Dauchez, M.; Derreumaux, P.; Lagant, P.; Vergoten, G. *J. Comput. Chem.* **1995**, *16* (2), 188.

(27) Brusau, E. V.; Narola, G. F.; Pedregosa, J. C.; Echeverria, C.; Punte, G. M. *J. Solid State Chem.* **1999**, *143*, 174.

(28) Csonka, C. I. *THEOCHEM* **2002**, *584*, 1.

(29) Keresztury, G.; Istvàn, K.; Sundius, T. *J. Phys. Chem. A* **2005**, *109*, 7938.

(30) Matsuhiro, B.; Conte, A. F.; Damonte, E. B.; Kolender, A. A; Matulewiz, M. C.; Mejias, E. G.; Pujol, C. A.; Zuniga, E. A. *Carbohydr. Res.* **2005**, *340*, 2392.

(31) Boggs, J. M.; Menikh, A.; Rangaraj, G. *Biophys. J.* **2000**, *78*, 874.

(32) Grant, D.; Long, W. F.; Moffat, C. F.; Williamson, F. B. *Biochem. J.* **1991**, *275*, 193.